

Uniqueness of infrared asymptotics in Landau gauge Yang-Mills theory

Christian S. Fischer¹ and Jan M. Pawłowski²

¹*Institut für Kernphysik, Technical University of Darmstadt,
Schlossgartenstraße 9, 64289 Darmstadt, Germany*

²*Institut für Theoretische Physik, Universität Heidelberg,
Philosophenweg 16, D-69120 Heidelberg, Germany.*

We uniquely determine the infrared asymptotics of Green functions in Landau gauge Yang-Mills theory. They have to satisfy both, Dyson-Schwinger equations and functional renormalisation group equations. Then, consistency fixes the relation between the infrared power laws of these Green functions. We discuss consequences for the interpretation of recent results from lattice QCD.

PACS numbers: 12.38.Aw,11.15.Tk,05.10.Cc,02.30.Rz

I. INTRODUCTION

In the past decade much progress has been made in the understanding of the low energy sector of QCD. This progress has been achieved both with continuum methods as well as lattice computations. In the continuum non-perturbative functional methods have been used: Dyson-Schwinger equations (DSEs) and functional renormalisation group equations (FRGs). Both frameworks are truly *ab initio* approaches in the sense that they can be derived rigorously from the full effective action of QCD, for reviews see [1, 2, 3, 4, 5, 6, 7]. Although both frameworks constitute an infinite hierarchy of coupled equations, they allow for the extraction of scaling laws for Green functions in the deep infrared [8, 9, 10, 11, 12]. These scaling laws are related to important properties of the low energy limit of QCD, such as confinement and chiral symmetry breaking.

A key building block relevant for the infrared behaviour of QCD are the ghost and gluon propagators. In Landau gauge the ghost dressing function gives access to the status of global gauge symmetry: an infrared diverging ghost unambiguously signals an unbroken symmetry corresponding to a well-defined global colour charge [13]. This is an integral part of the

Kugo-Ojima confinement scenario [14]. An infrared vanishing gluon propagator violates the Osterwalder-Schrader axiom of reflection positivity [15], and transverse gluons do not belong to the physical asymptotic state space of QCD. Finally, in Landau gauge one can construct a running coupling with a renormalisation group invariant combination of ghost and gluon dressing functions [8].

In Landau gauge QCD and in terms of correlation functions, the Kugo-Ojima confinement criterion is expressed as

$$p^2 \langle A(p)A(-p) \rangle \xrightarrow{p^2 \rightarrow 0} 0, \quad p^2 \langle C(p)\bar{C}(-p) \rangle \xrightarrow{p^2 \rightarrow 0} \infty, \quad (1)$$

with the gauge field A and the ghost/anti-ghost fields C, \bar{C} . An even stronger condition for the gluon propagator has been derived in a discretised version of Yang-Mills theory, where the infinite volume/continuum limit can be taken analytically: considerations on the impact of the (first) Gribov horizon on dressing functions led to Zwanziger's horizon condition [17, 18]

$$\langle A(p)A(-p) \rangle \xrightarrow{p^2 \rightarrow 0} 0, \quad (2)$$

which implies gluon confinement via positivity violation.

The behaviour (1) and (2) has first been seen in a DSE-study [8]. This result has been confirmed and extended within further DSE-computations, *e.g.* [10, 19, 20, 21], stochastic quantisation *e.g.* [9, 22] as well as FRG-computations [11, 23, 24, 25], for related work see also [26, 27, 28, 29]. In all these studies a non-renormalisation theorem for the ghost-gluon vertex [30] is used leading to

$$p^2 \langle A(p)A(-p) \rangle \rightarrow (p^2)^{2\kappa}, \quad p^2 \langle C(p)\bar{C}(-p) \rangle \rightarrow (p^2)^{-\kappa}, \quad (3)$$

with $\kappa \in [1/2, 1[$. It has been argued in [10] that (3) is the only consistent solution. Eq. (3) has been extended to a self-consistent solution of the (untruncated) tower of DSEs in continuum Yang-Mills theory [12]: for proper vertices $Z_{0,\text{as}}^{(2n,m)}$ with n ghost, n anti-ghost and m gluon legs the infrared asymptotics is given by

$$Z_{0,\text{as}}^{(2n,m)}(p^2) \sim (p^2)^{\kappa(2n,m)} \sim (p^2)^{(n-m)\kappa} \quad (4)$$

where κ is the exponent of the ghost dressing function ($n = 1, m = 0$) as defined in (3).

It is interesting to compare the continuum result (3) with results from lattice QCD [31, 32, 33, 34, 35, 36, 37, 38]. On the available finite volumes most lattice results for

the gluon propagator are compatible with (1) and (2). Extrapolations towards the infinite volume limit, *e.g.* [39], seem to agree with an infrared finite propagator, *i.e.*

$$p^2 \langle A(p)A(-p) \rangle \sim (p^2)^1, \quad (5)$$

see however [37] for an extrapolation leading to an infrared vanishing propagator.

The situation is much less clear for the ghost dressing function. Whereas some simulations give an infrared diverging ghost [36, 40], other authors interpret their results as pointing towards an infrared finite ghost dressing function [38], *i.e.*

$$\langle C(p)\bar{C}(-p) \rangle \sim (p^2)^0. \quad (6)$$

Clearly, (5) and (6) together do not agree with the continuum result (3). Instead, they have been proposed as a second possible solution of the continuum DSEs [38].

In this work we shall show that the infrared asymptotics of Landau gauge Yang-Mills is uniquely fixed by DSE and FRG. We first discuss the relations between these two sets of equations in the next section. Then a general infrared analysis of the DSEs for the ghost and gluon propagators as well as for the ghost-gluon vertex is performed. In the following section we repeat this analysis within the FRG, and show that (5), (6) cannot survive the infinite volume/continuum limit. In section V we show that self-consistency of DSEs and FRGs enforces the unique solution (4) for the infrared asymptotics of pure Yang-Mills theory. We briefly discuss the extension of the present analysis to QCD and the electro-weak sector of the standard model. In our concluding section we discuss the consequences of this result.

II. FUNCTIONAL RELATIONS

A quantum field theory or statistical theory can be defined uniquely in terms of its renormalised correlation functions. They are generated by the effective action Γ , the generating functional of 1PI Green functions. For the present work we consider pure Yang-Mills theory with the classical gauge fixed action

$$S_{\text{cl}} = \frac{1}{2} \int \text{tr} F^2 + \frac{1}{2\xi} \int (\partial_\mu A^\mu)^2 + \int \bar{C} \cdot \partial_\mu D_\mu \cdot C. \quad (7)$$

in the presence of an additional scale k , see [7] for a detailed discussion. The propagation is modified via k -dependent terms

$$\Delta S_k = \frac{1}{2} \int A_a^\mu R_{\mu\nu}^{ab} A_b^\nu + \int \bar{C}_a R^{ab} C_b, \quad (8)$$

where $R_{\mu\nu}^{ab}$ and R^{ab} are k -dependent regulator functions. Within the standard choice k is an infrared cut-off scale, and the functions R cut-off the propagation for momenta smaller than k . Here we also consider more general R that only have support at about the momentum scale k . Such regularisations allow for a scanning of the momentum behaviour of Green functions. The regularised effective action Γ_k is expanded in gluonic and ghost vertex functions and reads schematically

$$\Gamma_k[\phi] = \sum_{m,n} \frac{1}{m!n!^2} \Gamma_k^{(2n,m)} \bar{C}^n C^n A^m, \quad (9)$$

in an expansion about vanishing fields $\phi = (A, C, \bar{C})$. In (9) an integration over momenta and a summation over indices is understood. The effective action Γ_k satisfies functional relations such as the quantum equations of motion, the Dyson-Schwinger equations (DSEs); symmetry relations, the Ward or Slavnov-Taylor identities (STI); as well as RG or flow equations (FRGs). All these different equations relate to each other. Indeed, the Slavnov-Taylor identities are a projection of the quantum equations of motion, whereas flow equations can be read as differential DSEs, or DSEs as integrated flows. Written as a functional relation for the effective action Γ_k and specifying to pure YM theory, the DSE reads, *e.g.* [7]

$$\frac{\delta\Gamma_k}{\delta\phi}[\phi] = \frac{\delta S_{\text{cl}}}{\delta\phi}[\phi_{\text{op}}], \quad (10)$$

where the operators ϕ_{op} are defined as

$$\phi_{\text{op}}(x) = \int d^4y G_{\phi\phi_i}[\phi](x, y) \frac{\delta}{\delta\phi_i(y)} + \phi(x), \quad (11)$$

and

$$G_{\phi_1\phi_2}[\phi] = \left(\frac{1}{\Gamma_k^{(2)}[\phi] + R_k} \right)_{\phi_1\phi_2} \quad (12)$$

is the full field dependent propagator for a propagation from ϕ_1 to ϕ_2 , with $\phi = (A, C, \bar{C})$. The functional derivatives in (10) act on the corresponding fields and generate one loop and two loop diagrams in full propagators. The functional DSE (10) relates 1PI vertices, the expansion coefficients of Γ_k , to a set of one loop and two loop diagrams with full propagators and full vertices, but one classical vertex coming from the derivatives of S_{cl} . We emphasise that the DSE (10) only implicitly depends on the regularisation via the definition of the propagator in (12). It has the diagrammatic representation

$$\frac{\delta\Gamma_k[\phi]}{\delta A} = \frac{\delta S[\phi]}{\delta A} + \text{diagram 1} + \text{diagram 2} + \text{diagram 3}, \quad \frac{\delta\Gamma_k[\phi]}{\delta C} = \frac{\delta S[\phi]}{\delta C} + \text{diagram 4}$$

FIG. 1: Functional DSE for the effective action. Filled circles denote fully dressed field dependent propagators (12). Empty circles denote fully dressed field dependent vertices, dots denote field dependent bare vertices.

Fig. 1 shows the structure of the functional DSE (10). The rhs is given in powers of the field-dependent fully dressed propagator $G_{\phi\phi}[\phi]$, and its derivatives, as well as the field dependent bare vertices. The momentum scaling of Green functions is directly related to the scaling of these building blocks.

The flow equation for the effective action reads

$$\partial_t \Gamma_k[\phi] = \frac{1}{2} \int d^4p G_{ab}^{\mu\nu}[\phi](p, p) \partial_t R_{\mu\nu}^{ba}(p) - \int d^4p G_{ab}[\phi](p, p) \partial_t R^{ba}(p), \quad (13)$$

where $t = \ln k$. The flow (13) relates the cut-off scale derivative of the effective action to one loop diagrams with fully dressed field-dependent propagators. We can contrast the diagrammatic representation of the DSE in Fig. 1 with that of (13),

$$\partial_t \Gamma_k[\phi] = \frac{1}{2} \text{diagram 5} - \text{diagram 6}$$

FIG. 2: Functional flow for the effective action. Filled circles denote fully dressed field dependent propagators (12). Crosses denote the regulator insertion $\partial_t R$.

Fig. 2 shows the structure of the functional flow (13). The rhs is given by the field-dependent fully dressed propagator $G_{\phi\phi}[\phi]$ and the regulator insertion $\partial_t R$. Here, the momentum scaling of Green functions solely depends on the scaling of G and $\partial_t R$. If we choose the regulator function R such that it has the RG- and momentum scaling of the related two point function, the flow is RG-invariant [7], and only depends on full vertices and propagators, including the regulator term. The standard use of (13) is to take a regulator function $R(p^2)$ which tends towards a constant in the infrared and decays sufficiently fast in the ultraviolet, and hence implements an infrared cut-off. In the present context there is another interesting choice for R : let R only have support at momenta p about the scale k , and

$R \propto \Gamma_0^{(2)}$ at momenta $p^2 \approx k^2$. Then the regulator term does not change the theory, $\Gamma_k \simeq \Gamma_0$, and (13) only entails the (change of the) momentum dependence of Green functions of Γ_0 . This provides the resolution of the momentum dependence at p^2 of the full effective action Γ_0 directly from the flow equation at $k^2 = p^2$.¹ We shall detail this choice later. It is also worth noting that the relation between DSE and FRG is natural in a NPI formulation [7], which leads to a mixture of the scaling relations derived from (10) and (13).

In the present work we investigate the leading infrared behaviour of vertices and propagators constrained by consistency of (10) and (13). The crucial ingredient in the related consistency equations is the fact, that the DSEs derived from (10) also depend on bare or classical vertices whereas the flow equations derived from (13) solely depends on full vertices. This allows us to extract non-trivial information of the theory from a finite set of vertex DSEs and FRGs that would require a whole infinite tower of either DSEs or FRGs if restricting the analysis to either of the functional equations. We analyse the leading infrared behaviour of (10) and (13) for momenta and cut-offs

$$p^2, k^2 \ll \Lambda_{\text{QCD}}^2. \quad (14)$$

To that end we introduce dressing functions $Z_k^{(2n,m)}$ for one particle irreducible Green functions with n ghost, n anti-ghost and m gluon legs via

$$\Gamma_k^{(2n,m)}(p_1, \dots, p_{2n+m}) = Z_k^{(2n,m)}(p_1, \dots, p_{2n+m}) \mathcal{T}^{(2n,m)}(p_1, \dots, p_{2n+m}). \quad (15)$$

The expansion coefficients $\Gamma_k^{(2n,m)}$ of the effective action have been defined in (9). The $\mathcal{T}^{(2n,m)}$ denote the infrared leading tensor structure of the respective Green function, and carry their canonical momentum dimension. Then, following the IR analysis in [11, 25], the asymptotic vertex functions can be expanded about the leading asymptotics at vanishing cut-off $k = 0$:

$$Z_k^{(2n,m)}(p_1, \dots, p_{2n+m}) \simeq Z_{0,\text{as}}^{(2n,m)}(p_1, \dots, p_{2n+m}) \left(1 + \delta Z^{(2n,m)}(\hat{p}_1, \dots, \hat{p}_{2n+m})\right), \quad (16)$$

where $\hat{p}_i = p_i/k$, and the asymptotic infrared part $Z_{0,\text{as}}^{(2n,m)}$ only depends on ratios of monomials and possible logarithmic dependencies. Inserting the parameterisation (16) into the

¹ Such a single mode regulator cannot be used to solve the theory by successively integrating out degrees of freedom. However, it proves useful for studying fixed point solutions [41].

flow (13) and solving for $\delta Z^{(2n,m)}$ one can prove that $\delta Z^{(2n,m)}$ solely depends on \hat{p}_i . This suffices to fix the relations between the anomalous scalings of the vertex functions $Z_{0,\text{as}}^{(2n,m)}$ independent of the $\delta Z^{(2n,m)}$.

For our analysis we only have to know the global scaling behaviour for the dressing functions $Z_0^{(2n,m)}$, that is, modulo logarithmic scaling,

$$Z_{0,\text{as}}^{(2n,m)}(\lambda p_1, \dots, \lambda p_{2n+m}) = \lambda^{\kappa_{2n,m}} Z_{0,\text{as}}^{(2n,m)}(p_1, \dots, p_{2n+m}). \quad (17)$$

Specifically interesting for the Kugo-Ojima/Gribov-Zwanziger confinement scenario are the exponents $\kappa_{0,2}$ and $\kappa_{2,0}$ of the inverse gluon dressing function $Z^{(0,2)}$, and inverse ghost dressing function $Z^{(2,0)}$. The horizon conditions (1),(2) read

$$\kappa_{2,0} > 0 \quad \kappa_{0,2} < -1. \quad (18)$$

We close this section with the remark on the interpretation of the scaling analysis derived from the combined functional relations (10) and (13). In principle, such an analysis produces the most singular scaling of all diagrams involved and is neither sensitive to cancellations between different diagrams nor to cancellations within a given diagram. However, to affect the infrared behaviour of the Green functions in a consistent way, such cancellations have to work in the whole tower of DSEs and FRGs and therefore can only be driven by symmetries. In the present case we consider such a possibility as highly unlikely. We will come back to these points at the end of section V.

III. INFRARED ANALYSIS OF GHOST AND GLUON DSES

The Dyson-Schwinger equations for the ghost and gluon propagators are given diagrammatically in Fig. 3. The infrared behaviour of these propagators can be analysed as follows [9, 10, 12, 42]: We choose the external momentum scale p^2 , according to (14), to be much smaller than any other scale, *i.e.* $p^2 \ll \Lambda_{\text{QCD}}$, where $\Lambda_{\text{QCD}} \sim \mathcal{O}(200 \text{ MeV})$ is the non-perturbative scale of Yang-Mills theory generated via dimensional transmutation. The loop integrals on the right hand side of the DSEs are dominated by momentum configurations, where the internal loop momentum q is of the same order as the external momentum, *i.e.* $p^2 \sim q^2$. The reason for this well known behaviour is the appearance of at least one propagator in each loop with a denominator proportional to $(p-q)^2$. Thus a self-consistent solution

of the equations with small external momentum can be obtained by replacing all dressing functions inside the loops with their infrared asymptotic behaviour.

FIG. 3: Dyson-Schwinger equations for the gluon and ghost propagator. Filled circles denote dressed propagators and empty circles denote dressed vertex functions.

We illustrate this analysis at the example of the ghost DSE. For the sake of comparison with the literature we switch to the standard DSE notation, where the non-perturbative dressing of the propagators is denoted by propagator dressing functions $G(p^2)$ and $Z(p^2)$:

$$\frac{1}{Z_0^{(2,0)}(p^2)} = G(p^2), \quad \frac{1}{Z_0^{(0,2)}(p^2)} = Z(p^2), \quad (19)$$

and Zwanziger's horizon conditions (18) read

$$\lim_{p^2 \rightarrow 0} G(p^2) = \infty, \quad \lim_{p^2 \rightarrow 0} \frac{Z(p^2)}{p^2} = 0. \quad (20)$$

The DSE for the ghost propagator reads is given by

$$\frac{1}{G(p^2)} = \tilde{Z}_3 - g^2 N_c \int \frac{d^4 q}{(2\pi)^4} \frac{G(q^2) Z(l^2)}{p^2 q^2 l^2} p\mathcal{P}(l)q Z_0^{(2,1)}(p, q), \quad (21)$$

with the momentum routing $l = (q-p)$. The abbreviation $p\mathcal{P}(l)q$ denotes a contraction with the transverse momentum tensor $p\mathcal{P}(l)q = p_\mu P_{\mu\nu}(l) q_\nu$, and $Z_0^{(2,1)}(p, q)$ denotes the dressing

of the ghost-gluon vertex. The ghost renormalisation constant \tilde{Z}_3 absorbs all ultraviolet divergencies from the loop integral thus rendering the right hand side of the equation UV-finite. This can be made explicit within a momentum subtraction scheme. Here \tilde{Z}_3 is evaluated at a subtraction point $p^2 = \mu^2$, which we choose to be $\mu^2 = 0$. One obtains

$$\tilde{Z}_3 = \frac{1}{G(0)} + g^2 N_c \int \frac{d^4 q}{(2\pi)^4} \frac{3}{4} \frac{G(q^2)Z(q^2)}{q^4} Z_0^{(2,1)}(0, q). \quad (22)$$

and subsequently

$$\frac{1}{G(p^2)} = \frac{1}{G(0)} - g^2 N_c \int \frac{d^4 q}{(2\pi)^4} \left\{ \frac{G(q^2)Z(l^2)}{p^2 q^2 l^2} p \mathcal{P}(l) q Z_0^{(2,1)}(p, q) + \frac{3}{4} \frac{G(q^2)Z(q^2)}{q^4} Z_0^{(2,1)}(0, q) \right\}. \quad (23)$$

Now the integral is UV-finite and we replace the dressing functions in the loop by their infrared expansion in terms of the power laws

$$Z(p^2) \sim (p^2)^{-\kappa_{0,2}}, \quad G(p^2) \sim (p^2)^{-\kappa_{2,0}}, \quad Z_0^{(2,1)}(p, q) \sim (q^2)^{\kappa_{2,1}}, \quad (24)$$

The vertex function can be equally well represented by powers of (l^2) or, more realistically, by powers of $(p^2 + q^2 + l^2)$. The crucial point is, that after integration all powers of internal loop momenta will be transformed into powers of the only external scale p^2 for dimensional reasons. This can be seen easily for the expansion (24), which leads to integrals that can be performed employing

$$\int d^4 q \frac{(q^2)^a (l^2)^b}{q^2 l^2} = \pi^2 \frac{\Gamma(1+a)\Gamma(1+b)\Gamma(-a-b)}{\Gamma(1-a)\Gamma(1-b)\Gamma(2+a+b)} (p^2)^{a+b}. \quad (25)$$

Plugging (24) into (23), performing the integration and matching with the left hand side, $1/G(p^2) \sim (p^2)^{\kappa_{2,0}}$, we obtain two self-consistent solutions:

$$(p^2)^{\kappa_{2,0}} \sim \begin{cases} (p^2)^{-\kappa_{0,2} - \kappa_{2,0} + \kappa_{2,1}}, \\ (p^2)^0. \end{cases} \quad (26)$$

In the first case, the loop integral dominates the right hand side, and the constant $1/G(0)$ is cancelled by other terms (see [10] for a detailed discussion). In the second case this constant does not vanish and dominates the right hand side of the equation in the infrared. We thus end up with two possible conditions

$$\kappa_{2,0} \sim \begin{cases} -\frac{1}{2} \kappa_{0,2} + \frac{1}{2} \kappa_{2,1}, \\ 0, \end{cases} \quad (27)$$

from the ghost-DSE. Either $G(0)$ is divergent, in accordance with the horizon condition (20), or it is finite as proposed in [38] and violates (20). Strong arguments against the latter possibility have been discussed in [10, 43], where it has been concluded that $\kappa_{2,0} > 0$. For the sake of the argument, however, we will not use this result here but proceed by exploring the consequences of both options.

We would like to stress again that we could have obtained the solutions (27) without explicitly solving the loop integral: since the external momentum (p^2) is the only scale in our problem all powers of internal momenta in the loop have to translate into powers of external momentum after integration for dimensional reasons. Thus by simply counting the infrared exponents of all loop propagators and vertices we also arrive at (27).

We proceed by analysing the DSE for the gluon propagator. Schematically we can write this equation as

$$\frac{1}{Z(p^2)} = Z_3 + \Pi_{\text{tadpole}}(p^2) + \Pi_{\text{sunset}}(p^2) + \Pi_{\text{squint}}(p^2) + \Pi_{\text{gluonloop}}(p^2) + \Pi_{\text{ghostloop}}(p^2), \quad (28)$$

where the dressing loops appear in the same order as in Fig. 3. The static tadpole-term is absorbed in the process of renormalisation. We therefore have to analyse the infrared behaviour of the four remaining dressing loops. Counting IR-exponents in the loops we arrive at:

$$\begin{aligned} \Pi_{\text{sunset}}(p^2) &\sim (p^2)^{-3\kappa_{0,2} + \kappa_{0,4}} & \Pi_{\text{squint}}(p^2) &\sim (p^2)^{-4\kappa_{0,2} + 2\kappa_{0,3}} \\ \Pi_{\text{gluonloop}}(p^2) &\sim (p^2)^{-2\kappa_{0,2} + \kappa_{0,3}} & \Pi_{\text{ghostloop}}(p^2) &\sim (p^2)^{-2\kappa_{2,0} + \kappa_{2,1}}. \end{aligned} \quad (29)$$

The infrared leading term from the right hand side has to match the left hand side $1/Z(p^2) \sim (p^2)^{\kappa_{0,2}}$ of the DSE. We thus obtain the expression

$$\kappa_{0,2} = \min\left(0, -3\kappa_{0,2} + \kappa_{0,4}, -4\kappa_{0,2} + 2\kappa_{0,3}, -2\kappa_{0,2} + \kappa_{0,3}, -2\kappa_{2,0} + \kappa_{2,1}\right). \quad (30)$$

and subsequently

$$\kappa_{0,2} = \min\left(0, \frac{1}{4}\kappa_{0,4}, \frac{2}{5}\kappa_{0,3}, \frac{1}{3}\kappa_{0,3}, -2\kappa_{2,0} + \kappa_{2,1}\right), \quad (31)$$

as our final condition for the gluon exponent $\kappa_{0,2}$ from the gluon-DSE. In general we expect $\kappa_{0,2} < 0$ according to the Kugo-Ojima and horizon conditions (1), (20) and lattice QCD (see *e.g.* [39]). It is interesting to note that for negative $\kappa_{0,2}$ the contribution from the gluon loop, $1/3\kappa_{0,3}$, is never the leading one on the right hand side of (30), since it is always

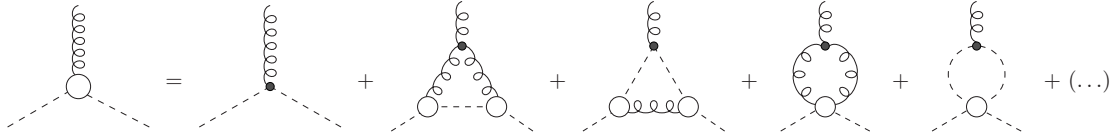


FIG. 4: Dyson-Schwinger equation for the ghost-gluon vertex, derived via Eq. (10). All internal propagators are taken to be fully dressed. The ellipsis denotes two-loop diagrams, which are not needed for our analysis.

dominated by the contribution from the squint diagram, $2/5\kappa_{0,3}$. Thus any truncation of the gluon-DSE that assumes a leading gluon loop (see *e.g.* [44, 45, 46]) is missing the dominant contribution in the infrared.

A further crucial ingredient is the DSE for the ghost-gluon vertex. One version is derived from the DSE for $\delta\Gamma/\delta A$, and is given diagrammatically in Fig. 4. Similarly to the ghost and gluon propagator DSE we arrive at

$$\kappa_{2,1} \leq \min\left(2\kappa_{2,0} + \kappa_{0,2}, 2\kappa_{0,2} + \kappa_{2,0}, \kappa_{2,2} - 2\kappa_{0,2}, \kappa_{4,0} - 2\kappa_{2,0}\right). \quad (32)$$

The inequality takes into account that the exponents of the two loop diagrams in the vertex-DSE may even be smaller than those of the one-loop diagrams considered in (32).² From (32) we conclude that

$$\kappa_{2,1} \leq 2\kappa_{2,0} + \kappa_{0,2}. \quad (33)$$

Eq. (33) together with the FRG-relation derived in the next section suffices to uniquely fix the relations between all $\kappa_{2n,m}$ in a closed form.

Based on the conditions (27) and (31) and the exact equality in (33) an infrared analysis of the DSEs for the three-gluon vertex and the four-gluon vertex has been performed in [12]. These results have been generalised to any Green function with n external ghost, n anti-ghost and m gluon legs:

$$Z_{0,\text{as}}^{(2n,m)}(p^2) \sim (p^2)^{(n-m)\kappa}, \quad (34)$$

with $\kappa = \kappa_{2,0} > 0$. This expression solves (27), (31) and any other condition from the higher DSEs. In addition it solves the Slavnov-Taylor identities. Important aspects of this

² $\kappa_{2,1}$ can be also determined from the DSE for $\delta\Gamma/\delta C$ or $\delta\Gamma/\delta\bar{C}$, see Fig. 1. However, the present analysis then turns out to be more complicated even though two loop terms are absent.

solution are discussed in detail in [3]. Two of the characteristic properties of (34) are: (i) contributions from ghost-loops always dominate the DSEs and (ii) it leads to IR-fixed points in the running couplings from the ghost-gluon (gh), three-gluon ($3g$) and four-gluon vertex ($4g$). These couplings are defined via

$$\alpha^{gh}(p^2) = \frac{g^2}{4\pi} [Z_0^{(2,1)}(p^2)]^2 G^2(p^2) Z(p^2), \quad (35a)$$

$$\alpha^{3g}(p^2) = \frac{g^2}{4\pi} [Z_0^{(0,3)}(p^2)]^2 Z^3(p^2), \quad (35b)$$

$$\alpha^{4g}(p^2) = \frac{g^2}{4\pi} [Z_0^{(0,4)}(p^2)] Z^2(p^2), \quad (35c)$$

where $Z_0^{-1} = Z_0^{(0,2)}$ and $G^{-1} = Z_0^{(2,0)}$. The vertex dressing functions $Z_0^{(2,1)}(p_1, p_2, p_3)$, $Z_0^{(0,3)}(p_1, p_2, p_3)$ and $Z_0^{(0,4)}(p_1, p_2, p_3)$ are evaluated at the symmetric momentum point $p_1^2 = p_2^2 = p_3^2 = p^2$, which make them functions of p^2 only.

From the tower of DSEs alone it is difficult to prove, that (34) is unique. One way to search for a second possible solution would be to assume $\kappa_{2,0} = 0$ and $\kappa_{0,2} = -1$ from the start, corresponding to the behaviour (5) and (6), as proposed in [38]. From Eqs. (27) and (31) one obtains consistency provided one of the three vertices is strongly divergent:

$$\kappa_{2,1} = -1, \quad \text{or} \quad \kappa_{0,3} = -5/2, \quad \text{or} \quad \kappa_{0,4} = -4. \quad (36)$$

In the next section we will show that all options (36) lead to inconsistencies in the functional renormalisation group equations.³ As discussed in section II, any solution of the tower of DSEs necessarily has to solve the tower of FRGs as well. This provides tight constraints on possible solutions, which are in fact sufficient to prove the uniqueness of (34), as we shall see.

IV. INFRARED ANALYSIS OF GHOST AND GLUON FLOWS

Now we repeat the infrared analysis within the FRG framework. We restrict ourselves to regulator functions of the form

$$R_k(p^2) = \Gamma_k^{(2)}(p^2) r(p^2/k^2), \quad (37)$$

³ Note that the second option together with (35b) leads to a strongly divergent running coupling, $\alpha^{3g} \sim 1/p^2$, which appears to the lattice results of [47].

where $\Gamma_k^{(2)}$ is the corresponding two point function $\Gamma_k^{(2,0)}$ for the ghost, and $\Gamma_k^{(0,2)}$ for the gluon. Regulator functions (37) guarantee the persistence of the standard RG-scalings in the presence of an IR cut-off, and are best-suited for the present studies. Within the parametrisation (16) and as a consequence of (37) propagators $G(p^2)$ take the asymptotic form

$$G(p^2) = \frac{1}{\Gamma_k^{(2)}(p^2)} \frac{1}{1+r(\hat{p}^2)} \simeq \frac{1}{\Gamma_{0,\text{as}}^{(2)}(p^2)} \frac{1}{1+\delta Z^{(2)}(\hat{p})} \frac{1}{1+r(\hat{p}^2)}. \quad (38)$$

Eq. (38) can be solely written in terms of \hat{p} and k -dependences. Then it reads

$$k^\kappa \frac{1}{\Gamma_{0,\text{as}}^{(2)}(\hat{p}^2)} \frac{1}{1+\delta Z^{(2)}(\hat{p})} \frac{1}{1+r(\hat{p}^2)}, \quad (39)$$

where κ is either $\kappa_{0,2}$ (gluon) or $\kappa_{2,0}$ (ghost). The same rescaling can be done with all vertex functions:

$$\Gamma_k^{(2n,m)}(p_1, \dots, p_{2n+m}) \simeq k^{-\kappa_{2n,m}} \Gamma_{0,\text{as}}^{(2n,m)}(\hat{p}_1, \dots, \hat{p}_{2n+m})(1 + \delta Z^{(2n,m)}(\hat{p}_1, \dots, \hat{p}_{2n+m})). \quad (40)$$

Another option for the infrared analysis is the choice of a regulator function R_k that only has support for momenta at about k^2 :

$$R_k(p^2) = \Gamma_0^{(2)}(p^2) \delta_\epsilon(p^2 - k^2) \quad (41)$$

where $\delta_\epsilon(x)$ is proportional to a smeared out δ -function at $x = 0$, the $\delta Z^{(2n,m)}$ only have support at momenta $p_i^2 \approx k^2$. With regulators (41), the momentum dependence of $\Gamma_k^{(2n,m)}$ agrees with that of $\Gamma_0^{(2n,m)}$. Only the *strength* of the two-point function $\Gamma_k^{(2)} \simeq \Gamma_0^{(2)}$ in the momentum window $p^2 \approx k^2$ is changed. In particular, the infrared power laws at $k \neq 0$ agree with those at $k = 0$. Therefore we can directly read-off the momentum-dependence at the momentum scale $p^2 = k^2$.

In turn, the general analysis with (40) provides additional information on the infrared cut-off flow. Within the parameterisation (40) integrated asymptotic flows for general vertices read

$$\delta Z^{(2n,m)}(\hat{p}_1, \dots, \hat{p}_{2n+m}) \simeq \int_0^k \frac{dk'}{k'} \left(\frac{1}{\Gamma_{0,\text{as}}^{(2n,m)}} \partial_t \Gamma_k^{(2n,m)} \right) (\hat{p}'_1, \dots, \hat{p}'_{2n+m}), \quad (42)$$

with possible sub-leading terms. Eq. (42) defines consistently renormalised finite DSEs [7]. In contrast to the DSEs (10) it solely depends on full vertices but also involves an integration

over the cut-off scale k . The term $\partial_t \Gamma^{(2n,m)}$ on the rhs of (42) is derived by taking $2n, m$ -derivatives of the rhs of the flow (13), leading to a sum of one loop diagrams with dressed vertices and dressed propagators. For vertices with $\kappa_{2n,m} < 0$ we have

$$\delta Z^{(2n,m)}(0, \dots, 0) = -1. \quad (43)$$

Eq. (43) simply entails that an infrared cut-off is present and the divergent infrared behaviour for $k = 0$ is suppressed. Trivially the infrared limit (43) only depends on \hat{p} . From (43) we derive a relation between the involved $\kappa_{i,j}$ with $i, j \leq n + 1, m + 2$ in the flow of $\Gamma_k^{(2n,m)}$ within an iteration about $\delta Z^{(2n,m)} \equiv 0$ on the rhs of (42). The analysis for $\kappa_{2n,m} \geq 0$ within the integrated flow (42) is a bit more involved in one to one correspondence to possible difficulties with bare terms in the DSEs. However, as outlined above we can also directly resolve the momentum behaviour from (13) with regulators (41), where these problems are absent. In fact this eliminates the possibility of solely dominating bare terms.

We proceed with the analysis of the propagator FRGs. They can be derived from Fig. 2 and are shown diagrammatically in Fig. 5.

We exemplify the analysis at the gluon propagator with $\kappa_{0,2} < 0$. As $\delta Z^{(0,2)}$ has to approach -1 , the momentum scaling of the k -integral has to precisely cancel that of $1/\Gamma_0^{(0,2)}(\hat{p} \rightarrow 0)$. On the rhs of (42) we can iterate the full $\Gamma_k^{(2n,m)}$ about those at $k = 0$, $\Gamma_{0,\text{as}}^{(2n,m)}$. Consequently we can simply sum over the $\kappa_{2n,m}$ to identify the leading \hat{p} -behaviour. With the regulator (41) this follows directly, as within this choice we have $\Gamma_k^{(2n,m)} \propto \Gamma_{0,\text{as}}^{(2n,m)}$ in the flow. Then the relations between the $\kappa_{2n,m}$ follow from simple counting of powers of momenta. From the flow equation for the gluon propagator we derive the relation

$$\kappa_{0,2} = \min\left(2\kappa_{2,1} - 2\kappa_{2,0}, 2\kappa_{0,3} - 2\kappa_{0,2}, \kappa_{0,4} - \kappa_{0,2}, \kappa_{2,2} - \kappa_{2,0}\right), \quad (44)$$

which can be solved for $\kappa_{0,2}$,

$$\kappa_{0,2} = \min\left(2\kappa_{2,1} - 2\kappa_{2,0}, \frac{2}{3}\kappa_{0,3}, \frac{1}{2}\kappa_{0,4}, \kappa_{2,2} - \kappa_{2,0}\right). \quad (45)$$

Eq. (45) is already sufficient to rule out all three options in (36). Indeed, if we insert (36) into (45) we arrive at

$$\kappa_{0,2} \leq \begin{cases} -2, \\ -\frac{5}{3}, \\ -2, \end{cases} \quad (46)$$

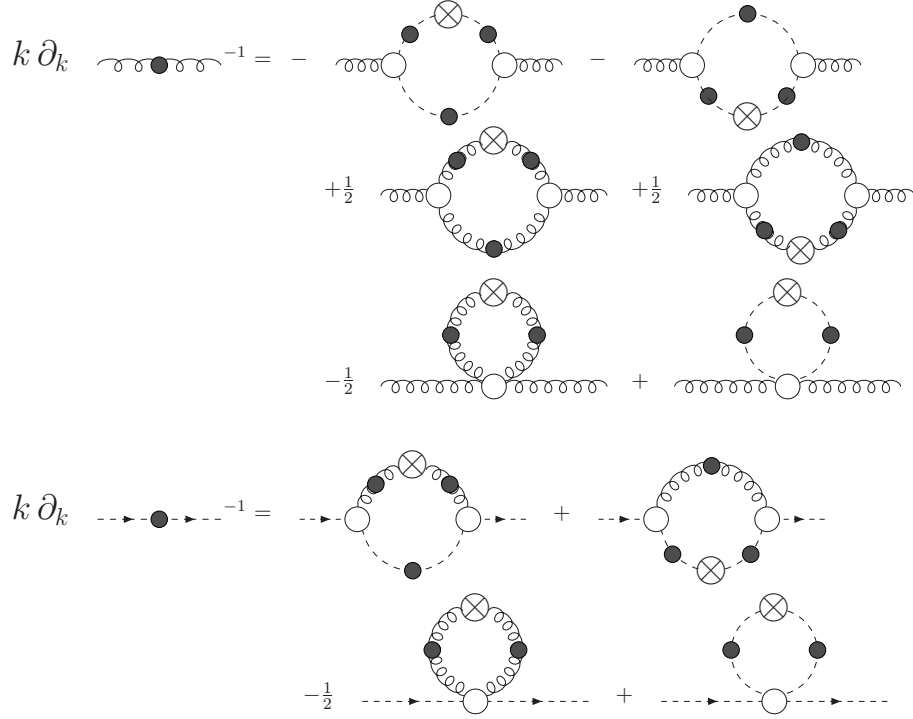


FIG. 5: Functional renormalisation group equations for the gluon and ghost propagator. Filled circles denote dressed propagators and empty circles denote dressed vertex functions. Crosses indicate insertions of the infrared cutoff function.

for the three options. However, (36) goes with $\kappa_{0,2} = -1$. The behaviour (5) and (6), proposed in [38], is therefore ruled out.

Now we use the combined DSE-FRG analysis to uniquely determine the κ 's without any further input. We shall see that a self-consistent solution leads to

$$\kappa_{2,1} = 0. \quad (47)$$

To that end we also discuss the derivation of the κ 's for the ghost-propagator and the ghost-gluon vertex. For general regulators the infrared analysis for the ghost propagator is intricate and we defer the reader to [11, 25]. With the choice (41) the result follows directly from the flow of the ghost propagator. Analogously to (45) we get from Fig. 5

$$\kappa_{2,0} = \min\left(\kappa_{2,1} - \frac{1}{2}\kappa_{0,2}, \kappa_{2,2} - \kappa_{0,2}, \frac{1}{2}\kappa_{4,0}\right). \quad (48)$$

The FRG relations (45),(48) as well as the DSE relations (27),(31) for $\kappa_{2,0}$ and $\kappa_{0,2}$ are not closed as they also depend on vertex kappa's. The ghost-gluon vertex comprises the crucial

information. It is protected by non-renormalisation which turns out to be powerful enough to fix the whole system completely. Its flow is given by all one loop diagrams with regulator insertions and full vertices (up to 5 point vertices) with one external gluon line and one ghost and anti-ghost line. It reads schematically

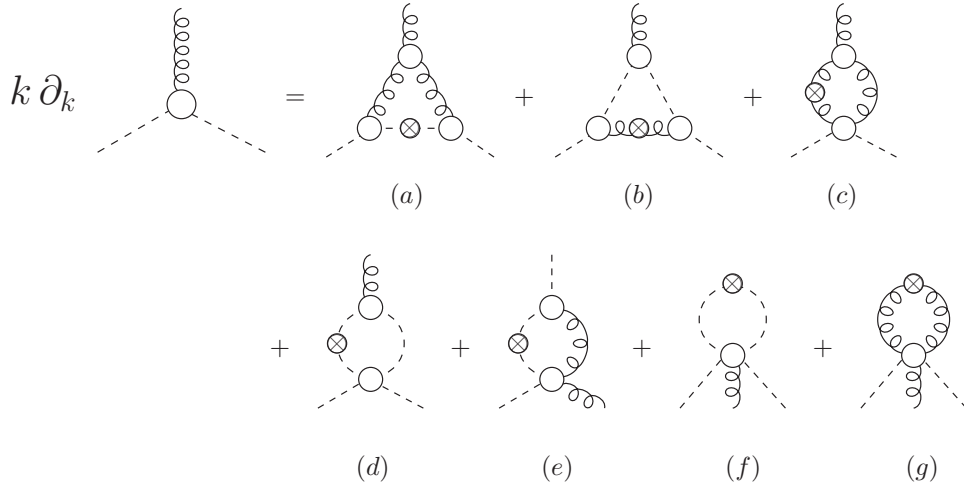


FIG. 6: Functional renormalisation group equations for the ghost gluon vertex. All propagators and vertices are fully dressed. Only one possible insertion of the infrared cutoff function per diagram is shown.

The infrared analysis of Fig. 6 with (42), or alternatively employing (41), leads to

$$\kappa_{2,1} = \min\left(2\kappa_{0,2} + \kappa_{2,0} - \kappa_{0,3}, \frac{1}{2}\kappa_{0,2} + \kappa_{2,0}, \kappa_{0,3} + \kappa_{2,2} - 2\kappa_{0,2}, \kappa_{4,1} - \kappa_{2,0}, \kappa_{2,3} - \kappa_{0,2}\right), \quad (49)$$

from the diagrams (a), (b), (c), (f), (g) respectively. The diagrams (d),(e) involve exactly one ghost gluon vertex and the related anomalous scaling cancels on both sides of Fig. 6. The surviving κ 's cannot be negative, as this spoils self-consistency of the integrated flow. Hence (d),(e) lead to the constraints

$$\kappa_{4,0} - 2\kappa_{2,0} \geq 0, \quad (50a)$$

$$\kappa_{2,2} - \kappa_{0,2} - \kappa_{2,0} \geq 0. \quad (50b)$$

Additionally the non-renormalisation of the ghost-gluon vertex [30] constrains

$$\kappa_{2,1} \leq 0, \quad (51)$$

as at least one tensor structure of the ghost-gluon vertex has a finite dressing. From the

second term on the rhs of (49) we extract

$$\kappa_{2,1} \leq \frac{1}{2}\kappa_{0,2} + \kappa_{2,0}. \quad (52)$$

We insert (52) in the first term of (44) and arrive at $\kappa_{0,2} \leq \kappa_{0,2}$. Consequently the bound in (52) has to be saturated and

$$\kappa_{2,1} = \frac{1}{2}\kappa_{0,2} + \kappa_{2,0}. \quad (53)$$

The DSE-analysis leads to the constraint $\kappa_{2,1} \leq \kappa_{0,2} + 2\kappa_{2,0}$, (33). With (53) this turns into $\kappa_{2,1} \leq 2\kappa_{2,1}$. As $\kappa_{2,1} \leq 0$, (51), we arrive at the unique solution

$$\kappa_{2,1} = 0, \quad (54)$$

accompanied by the relation

$$\kappa_{0,2} = -2\kappa_{2,0}, \quad (55)$$

for the dressing of ghost and gluon propagators in agreement with [8].

V. UNIQUENESS OF INFRARED ASYMPTOTICS

The analysis of the last two sections for the propagators and the ghost-gluon vertex can be extended to all $\kappa_{n,m}$. We first derive the relations for the purely gluonic three and four point functions. The flow of three and four gluon vertices is given by all one loop diagrams with regulator insertions and full vertices (up to 5 and 6 point vertices respectively). For the three gluon vertex this reads schematically

Using Fig. 7 we arrive at

$$\kappa_{0,3} = \min\left(\frac{3}{2}\kappa_{0,2}, 3\kappa_{2,1} - 3\kappa_{2,0}, \kappa_{2,2} + \kappa_{2,1} - 2\kappa_{2,0}, \kappa_{2,3} - \kappa_{2,0}, \kappa_{0,5} - \kappa_{0,2}\right), \quad (56)$$

from the diagrams (a), (b), (d), (e), (f). The diagram (c) leads to the constraint

$$\kappa_{0,4} - 2\kappa_{0,2} \geq 0, \quad (57)$$

which already restricts the singular behaviour of the four gluon vertex. We also remark that (56) puts a simple upper bound on $\kappa_{0,3}$, namely

$$\kappa_{0,3} \leq \frac{3}{2}\kappa_{0,2}. \quad (58)$$

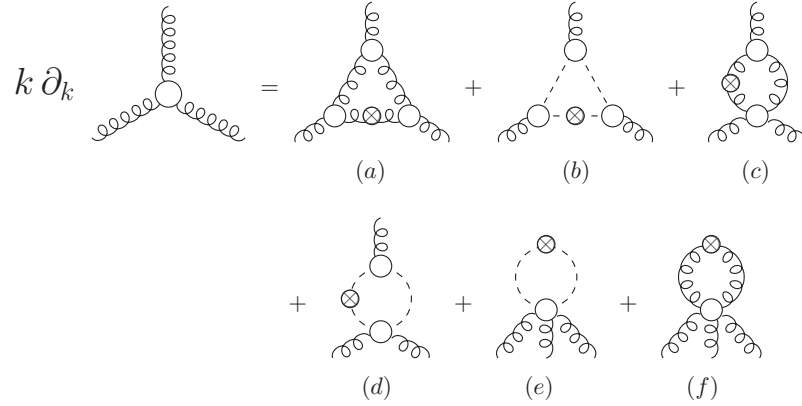


FIG. 7: Functional renormalisation group equations for the three gluon vertex. All internal propagators are taken to be fully dressed. Only one possible insertion of the infrared cutoff function per diagram is shown.

This bound is the natural scaling of the vertex in the presence of a fixed point for the coupling constant α_s . Note however that a priori not all couplings as defined in (35) run to a fixed point.

The same analysis can be done for the four gluon vertex. Its flow reads schematically

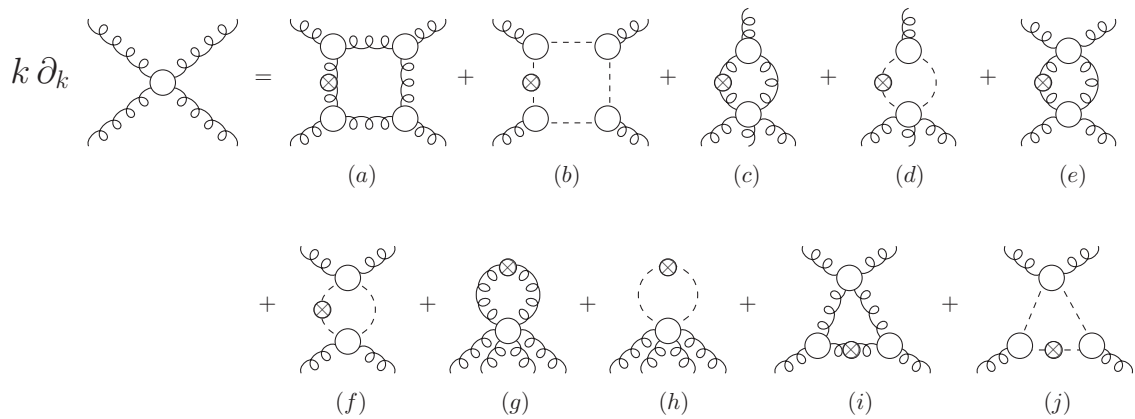


FIG. 8: Functional renormalisation group equations for the four gluon vertex. All internal propagators are taken to be fully dressed. Only one possible insertion of the infrared cutoff function per diagram is shown.

Similarly as for the three gluon vertex we derive from Fig. 8 the anomalous scaling of the

four gluon vertex

$$\kappa_{0,4} = \min\left(4\kappa_{0,3} - 4\kappa_{0,2}, 4\kappa_{2,1} - 4\kappa_{2,0}, \kappa_{0,5} + \kappa_{0,3} - 2\kappa_{0,2}, \kappa_{2,3} + \kappa_{2,1} - 2\kappa_{2,0}, 2\kappa_{0,2}, 2\kappa_{2,2} - 2\kappa_{2,0}, \kappa_{0,6} - \kappa_{0,2}, \kappa_{2,4} - \kappa_{2,0}, \kappa_{2,2} + 2\kappa_{2,1} - 3\kappa_{2,0}\right), \quad (59)$$

from the diagrams (a), ..., (h), (j) respectively. The diagram (i) leads to the constraint

$$2\kappa_{0,3} - 3\kappa_{0,2} \geq 0. \quad (60)$$

The first term in the second line of (59) puts a bound on $\kappa_{0,4}$,

$$\kappa_{0,4} \leq 2\kappa_{0,2}. \quad (61)$$

Together with the constraint (57) this gives the unique solution

$$\kappa_{0,4} = 2\kappa_{0,2}, \quad (62)$$

and

$$\kappa_{0,3} = \frac{3}{2}\kappa_{0,2}. \quad (63)$$

Note that the scaling laws (62),(63) are already generated by the diagrams involving ghosts. Indeed, this is valid for all proper vertices and leads to the unique solution

$$\kappa_{2n,m} = (n - m)\kappa, \quad \text{with } \kappa = \kappa_{2,0}, \quad (64)$$

which we now prove: first we observe that with (64) all diagrams in the FRG have the same leading infrared asymptotics. Let us assume for a moment that (64) is not true for all proper vertices. Then at least one vertex has

$$\kappa_{2n_0,m_0} < (n_0 - m_0)\kappa. \quad (65)$$

The vertex $\Gamma^{(2n_0,m_0)}$ occurs in diagrams of FRG for lower vertex functions $\Gamma^{(2n,m)}$ with $n_0 - n = 1$ or $m_0 - m = 1$. Necessarily also these vertices satisfy (65) and disagree with (64). Within an iteration this enforces that *all* vertices with $n \leq n_0$ and $m \leq m_0$ satisfy (65), in particular $\kappa_{0,4}, \kappa_{0,3}, \kappa_{0,2}, \kappa_{2,1}, \kappa_{2,0}$. This contradicts the uniqueness of the results (54), (55),(62),(63) derived above, and hence proves (64).

For the special case of the propagators this relation has been already derived in [8, 10] with the help of additional physical constraints. In [12] the self-consistency of (64) for the

whole tower of vertex DSEs has been shown. The dominance of ghost loops in the tower of DSEs is equivalent to the dominance of the Faddeev-Popov determinant over the Yang-Mills action, as proposed in [22]. In the present work we were able to extend these results to a proof of uniqueness based on a self-consistency analysis of the quantum equations of motion.

The above results hinges on a key structure valid for general theories in the presence of a single dynamical scale, and follows already from the structure of the functional DSE (10), Fig. 1 and FRG (13), Fig. 2: any vertex DSE comprises a sum of diagrams proportional to a subset of the bare vertices of the theory at hand. Consistency with the FRG, which only depends on dressed vertices, requires that in all vertex DSEs at least one of these vertices, if dressed, has $\kappa_{\text{vertex}} = 0$. In Landau gauge Yang-Mills this is the ghost-gluon vertex. In general the above criterion leads to more than one vertex with $\kappa_{\text{vertex}} = 0$.

As an example for this general pattern we extend the pure gauge theory analysis to a YM-Higgs theory. The functional DSE and FRG can be read-off from (10),(13) with $\phi = (A, C, \bar{C}, h)$ and an additional Higgs action $S_{\text{higgs}} = \frac{1}{2} \int (D_\mu h)^2 + V[h]$. Under the assumption of a single, dynamical mass scale we deduce a unique relation for a general vertex function $\Gamma^{(2n,m,2l)}$ with n ghost, n anti-ghost, m gluon, h Higgs lines,

$$\kappa_{2n,m,h} = (n - m)\kappa \quad \text{with} \quad \kappa = \kappa_{2,0,0}. \quad (66)$$

In particular it follows that the Higgs propagator has a constant dressing: $\kappa_h = \kappa_{0,0,2} = 0$, as well as the ϕ^4 -coupling $\kappa_{0,0,4} = 0$ required by the presence of vertices with constant dressings in all DSEs. Note that $\kappa_{2n,m,l} = 0$ includes logarithmic scaling. Eq. (66) is only valid in the symmetric phase. In the spontaneously broken phase we expect a massive gauge field propagator, $\kappa_{0,2,0} = -1$, and massive Higgs propagators, $\kappa_h = -1$. Furthermore, as a positive $\kappa \geq 0$ for the ghost signals an unbroken (colour) symmetry, we conclude $\kappa \leq 0$ in agreement with the converse of the Higgs theorem [14]. Due to the additional mass scale some if not all other vertices may scale canonically, *i.e.* $\kappa_{2n,m,h} = 0$. The present infrared analysis then shows consistently $\kappa_{2n,m,h} \geq 0$, no singular scaling occurs. This is in marked contrast to massless Yang-Mills theory.

In the case of full QCD, including dynamical quarks, the present infrared analysis has interesting consequences which shall be published elsewhere. Finally we discuss the caveat mentioned at the end of section II. From the above analysis it is clear non-trivial cancellations always have to occur in an infinite sub-set of diagrams. It is hard to see which

symmetry should be responsible for such a behaviour, as constraints from gauge symmetry, *i.e.* STIs, are respected by the solution (64).

VI. CONCLUSIONS

In this work we used Dyson-Schwinger equations (DSEs) and functional renormalisation group equations (FRGs) to analyse the infrared behaviour of proper vertices of $SU(N_c)$ Yang-Mills theory. We have shown that the structure of these functional relations is sufficiently different to generate tight constraints for infrared anomalous dimensions of these vertices. The caveats of this construction have been discussed at the end of sections II and V. The constraints are powerful enough to enforce a unique solution (4),(64) for the infrared behaviour of proper vertices in the presence of only one external scale. Thus the Kugo-Ojima criterion (1) is satisfied ensuring a well-defined global colour charge. A further consequence is the fixed point behaviour of the running coupling in the infrared, since this behaviour is implied by the solution (4) via the non-perturbative definitions in Eqs. (35). In turn the proposal (5), (6) in [38] is excluded.

We emphasise that both, the similarities as well as the differences of DSEs and FRG were crucial for our results. This structure is certainly useful beyond the present investigation, for example if devising truncation schemes. Implicitly this was already used for enhancing the respective reliability: the coinciding results for the infrared asymptotics from DSE [8, 9, 10, 12] and FRG [11, 23, 25] are non-trivial as the functional equations are sufficiently different.

The present consistency analysis not only uniquely fixes the infrared asymptotics but also excludes certain truncation schemes of DSEs and FRGs: *e.g.* we have shown that truncation schemes of the gluon-DSE in Landau gauge Yang-Mills relying on an infrared leading behaviour of the gluonic one-loop diagram, as *e.g.* assumed in [45, 46] miss the leading infrared behaviour. In addition, truncation schemes that assume all terms in the gluon-DSE to be equally leading [44] are excluded as well.

It would be desirable to reproduce (4) from lattice QCD. To this end one has to address some caveats in comparing infrared results from the lattice with those of a continuum approach. Lattice simulations are necessarily performed at finite volume and finite lattice spacing and one has to carefully perform both an infinite volume and continuum limit extrap-

olation. These procedures are currently under debate [37, 39, 48, 49, 51]. It is interesting, however, that the procedure of [37] gives $\kappa_{0,2} \approx -1.04$ in agreement with (1). Unfortunately direct lattice calculations in the infrared scaling region $p < 100$ MeV are extremely expensive in terms of CPU-time and have not yet been performed in four dimensional Yang-Mills theory. This is different in three dimensions, where lattice results are in good agreement with the corresponding power-law analysis in the continuum [50].

Furthermore, gauge fixing is implemented differently. In the continuum theory one uses either the Faddeev-Popov method [52] or stochastic gauge fixing [22]), whereas on the lattice a gauge fixing functional is extremised. Due to the presence of Gribov copies this might affect the infrared behaviour of Green functions. These effects are currently under investigation in the continuum [22] and on the lattice [31, 33, 35, 53, 54, 55]. The effects seem to be much stronger for the ghost than for the gluon propagator. This nicely corresponds to the fact that lattice and continuum solutions agree much better for the gluon than for the ghost.

The present analysis can be extended to full QCD, and reveals an interesting structure. Related results will be published elsewhere.

Acknowledgements

CF is grateful to J. Papavassiliou and J. Rodriguez-Quintero for interesting discussions. We thank R. Alkofer, H. Gies, D.F. Litim and L. von Smekal for a critical reading of the manuscript and useful discussions. This work has been supported by the Deutsche Forschungsgemeinschaft (DFG) under contract Fi 970/7-1 and GI328/1-2.

-
- [1] C. D. Roberts and A. G. Williams, *Prog. Part. Nucl. Phys.* **33** (1994) 477 [hep-ph/9403224].
 - [2] R. Alkofer and L. von Smekal *Phys. Rept.* **353** (2001) 281 [hep-ph/0007355].
 - [3] C. S. Fischer *J. Phys. G: Nucl. Part. Phys.* **32** (2006) R253–R291 [hep-ph/0605173].
 - [4] D. F. Litim and J. M. Pawłowski, hep-th/9901063.
 - [5] J. Berges, N. Tetradis and C. Wetterich, *Phys. Rept.* **363** (2002) 223 [hep-ph/0005122].
 - [6] J. Polonyi, *Central Eur. J. Phys.* **1** (2004) 1 [hep-th/0110026].
 - [7] J. M. Pawłowski, [hep-th/0512261].
 - [8] L. von Smekal, R. Alkofer, and A. Hauck *Phys. Rev. Lett.* **79** (1997) 3591–3594 [hep-ph/9705242].

- [9] D. Zwanziger *Phys. Rev.* **D65** (2002) 094039 [hep-th/0109224].
- [10] C. Lerche and L. von Smekal *Phys. Rev.* **D65** (2002) 125006, [hep-ph/0202194].
- [11] J. M. Pawłowski, D. F. Litim, S. Nedelko, and L. von Smekal *Phys. Rev. Lett.* **93** (2004) 152002 [hep-th/0312324].
- [12] R. Alkofer, C. S. Fischer, and F. J. Llanes-Estrada *Phys. Lett.* **B611** (2005) 279–288 [hep-th/0412330].
- [13] T. Kugo, [hep-th/9511033].
- [14] T. Kugo and I. Ojima *Prog. Theor. Phys. Suppl.* **66** (1979) 1.
- [15] K. Osterwalder and R. Schrader *Commun. Math. Phys.* **31** (1973) 83–112.
- [16] S. Mandelstam, *Phys. Rev. D* **20**, 3223 (1979).
- [17] D. Zwanziger *Nucl. Phys.* **B364** (1991) 127–161.
- [18] D. Zwanziger *Nucl. Phys.* **B399** (1993) 477–513.
- [19] C. S. Fischer and R. Alkofer *Phys. Lett.* **B536** (2002) 177–184 [hep-ph/0202202].
- [20] C. S. Fischer and R. Alkofer, *Phys. Rev. D* **67** (2003) 094020 [hep-ph/0301094].
- [21] R. Alkofer, W. Detmold, C. S. Fischer and P. Maris, *Phys. Rev. D* **70**, 014014 (2004) [hep-ph/0309077].
- [22] D. Zwanziger *Phys. Rev.* **D69** (2004) 016002 [hep-ph/0303028].
- [23] C. S. Fischer and H. Gies *JHEP* **10** (2004) 048 [hep-ph/0408089].
- [24] D. F. Litim, J. M. Pawłowski, S. Nedelko and L. V. Smekal, hep-th/0410241.
- [25] J. M. Pawłowski, D. F. Litim, S. Nedelko and L. von Smekal, *AIP Conf. Proc.* **756** (2005) 278 [hep-th/0412326].
- [26] U. Ellwanger, M. Hirsch and A. Weber, *Z. Phys. C* **69** (1996) 687 [arXiv:hep-th/9506019].
- [27] U. Ellwanger, M. Hirsch and A. Weber, *Eur. Phys. J. C* **1** (1998) 563 [hep-ph/9606468].
- [28] B. Bergerhoff and C. Wetterich, *Phys. Rev. D* **57** (1998) 1591 [hep-ph/9708425].
- [29] J. Kato, hep-th/0401068.
- [30] J. C. Taylor *Nucl. Phys.* **B33** (1971) 436–444.
- [31] A. Cucchieri *Nucl. Phys.* **B508** (1997) 353–370 [hep-lat/9705005].
- [32] D. B. Leinweber, J. I. Skullerud, A. G. Williams and C. Parrinello [UKQCD Collaboration], *Phys. Rev. D* **60** (1999) 094507 [Erratum-ibid. *D* **61** (2000) 079901] [hep-lat/9811027].
- [33] C. Alexandrou, P. de Forcrand, and E. Follana *Phys. Rev.* **D63** (2001) 094504 [hep-lat/0008012].

- [34] K. Langfeld, H. Reinhardt and J. Gattnar, *Nucl. Phys. B* **621** (2002) 131 [hep-ph/0107141].
- [35] S. Furui and H. Nakajima *Phys. Rev.* **D70** (2004) 094504.
- [36] A. Sternbeck, E. M. Ilgenfritz, M. Mueller-Preussker, and A. Schiller *Phys. Rev.* **D72** (2005) 014507 [hep-lat/0506007].
- [37] P. J. Silva and O. Oliveira, hep-lat/0511043.
- [38] P. Boucaud *et al.*, hep-ph/0507104.
- [39] F. D. R. Bonnet, P. O. Bowman, D. B. Leinweber, A. G. Williams, and J. M. Zanotti *Phys. Rev.* **D64** (2001) 034501 [hep-lat/0101013].
- [40] J. Gattnar, K. Langfeld, and H. Reinhardt *Phys. Rev. Lett.* **93** (2004) 061601 [hep-lat/0403011].
- [41] D. F. Litim, in preparation.
- [42] W. Schleifenbaum, M. Leder, and H. Reinhardt *Phys. Rev.* **D73** (2006) 125019 [hep-th/0605115].
- [43] P. Watson and R. Alkofer *Phys. Rev. Lett.* **86** (2001) 5239 [hep-ph/0102332].
- [44] J. C. R. Bloch, *Few Body Syst.* **33** (2003) 111 [hep-ph/0303125].
- [45] A. C. Aguilar and A. A. Natale *Int. J. Mod. Phys.* **A20** (2005) 7613–7632 [hep-ph/0405024].
- [46] A. C. Aguilar and A. A. Natale *JHEP* **08** (2004) 057, [hep-ph/0408254].
- [47] P. Boucaud *et al.* *JHEP* **04** (2003) 005 [hep-ph/0212192].
- [48] A. Cucchieri and T. Mendes [hep-lat/0602012].
- [49] P. Boucaud *et al.* [hep-lat/0602006].
- [50] A. Cucchieri, T. Mendes, and A. R. Taurines *Phys. Rev.* **D67** (2003) 091502 [hep-lat/0302022].
- [51] T. Tok, K. Langfeld, H. Reinhardt, and L. von Smekal *PoS LAT2005* (2006) 334 [hep-lat/0509134].
- [52] L. D. Faddeev and V. N. Popov *Phys. Lett.* **B25** (1967) 29–30.
- [53] P. J. Silva and O. Oliveira *Nucl. Phys.* **B690** (2004) 177–198 [hep-lat/0403026].
- [54] I. L. Bogolubsky, G. Burgio, M. Muller-Preussker, and V. K. Mitrjushkin, hep-lat/0511056.
- [55] A. Y. Lokhov, O. Pene, and C. Roiesnel, hep-lat/0511049.